



## Original Article

The  $\mu$ -synthesis and analysis of water level control in steam generators

Ahmad Salehi, Mohammad Hosein Kazemi\*, Omid Safarzadeh

Electrical Engineering Department, Shahed University, Tehran, Iran

## ARTICLE INFO

## Article history:

Received 16 May 2018

Received in revised form

18 August 2018

Accepted 26 September 2018

Available online 27 September 2018

## Keywords:

Robust control

Steam generator

Uncertainty modeling

 $\mu$ -synthesis

## ABSTRACT

The robust controller synthesis and analysis of the water level process in the U-tube system generator (UTSG) is addressed in this paper. The parameter uncertainties of the steam generator (SG) are modeled as multiplicative perturbations which are normalized by designing suitable weighting functions. The relative errors of the nominal SG model with respect to the other operating power level models are employed to specify the weighting functions for normalizing the plant uncertainties. Then, a robust controller is designed based on  $\mu$ -synthesis and D-K iteration, and its stability robustness is verified over the whole range of power operations. A gain-scheduled controller with  $H_\infty$ -synthesis is also designed to compare its robustness with the proposed controller. The stability analysis is accomplished and compared with the previous QFT design. The  $\mu$ -analysis of the system shows that the proposed controller has a favorable stability robustness for the whole range of operating power conditions. The proposed controller response is simulated against the power level deviation in start-up and shutdown stages and compared with the other concerning controllers.

© 2018 Korean Nuclear Society, Published by Elsevier Korea LLC. This is an open access article under the CC BY-NC-ND license (<http://creativecommons.org/licenses/by-nc-nd/4.0/>).

## 1. Introduction

Creating the steam to drive the turbine in nuclear plants are the important function of the steam generators (SG). Water level control has a critical role in the SG for preventing some specific problems such as overflowing of the steam equipment when the water level is too high, and declining the recirculation efficacy in the case of low water level. The system parameter variations and its non-linearity are caused that the SG to be a time varying system and highly complex. The control problem of the water level in the SG is known as a main contributor to plant unavailability [1–3].

Several researchers have been assayed to develop an effective controller for the SG water level system, and numerous encouraged controllers have been introduced. A linear model with varying parameter is presented by Ref. [1], to describe the dynamics of the SG over the whole power level range. This model has been mostly utilized for water-level control synthesis in the SGs. It is employed for designing a PI-like controller to stabilize the water level system in the case of low power level by Ref. [4]. It is also used to design a PI-based compensator to counteract the reverse response of the SG

in Ref. [5]. A model predictive control (MPC) technique is addresses in Ref. [6] by defining the objective functions to penalize the supplying water flowrate deviations, the restrictions on the water level magnitude, and the output error. It indicates that the MPC performance can be enhanced considerably if the power changes are known. In Ref. [7], a generalized predictive control is proposed to encounter with the model perturbations by using parameter estimation in a recursive algorithm manner. The same objective is achieved in Ref. [8], where the linear matrix inequality is used to solve an online optimization problem. For overcoming the non-minimum phase phenomenon of the SG model, a dynamical sliding mode scheme (DSMC) is suggested in Ref. [9] to design a pole-placement controller. Its pole placement approach is used based on the assumption that all system states are available. In Ref. [10], the internal model control (IMC) scheme is used to design a controller in the feedback loop, and a forward compensator is also designed in order to reject the disturbance effects. It applies its proposed controller in a gain-scheduled manner to achieve the desired performance for regulating the SG water level at the whole range of power demands. Although the methods based on gain-scheduling deliver an acceptable performance, however, they cannot guarantee the overall stability of the system. The quantitative feedback theory (QFT) is utilized in Ref. [11] to synthesis a robust water level compensator based on the loop shaping with

\* Corresponding author.

E-mail addresses: [ahmadsalehi.shahed@gmail.com](mailto:ahmadsalehi.shahed@gmail.com) (A. Salehi), [kazemi@shahed.ac.ir](mailto:kazemi@shahed.ac.ir) (M.H. Kazemi), [safarzadeh@shahed.ac.ir](mailto:safarzadeh@shahed.ac.ir) (O. Safarzadeh).

shifted robust bounds to counteract the non-minimum phase activity of the system.

On the other side, some researches have been accomplished to apply the artificial intelligence techniques in control of U-tube SG (UTSG) water level, such as adaptive neuro-fuzzy, model-based predictive, adaptive critic-based, neuro-fuzzy, genetic fuzzy, and fuzzy gain-scheduled neural controllers [12–16]. Extreme learning machines (ELM) are also proposed in Ref. [17] for modeling the UTSG system in offline and online modes and identifying the water level for system monitoring, diagnostics, and control applications. The better learning ability is achieved because of the randomness of the ELM compared to the other classical schemes.

One of the main control objective of the UTSG water level is the robustness of the system against the power operation deviations. In Ref. [18],  $H_\infty$  controllers are designed at nine various operating points utilizing gain-scheduling to obtain a global water-level controller. In Ref. [19], a robust  $H_\infty$  controller is presented base on the ten identified models for the SG engaging the loop-shaping  $H_\infty$  synthesis, and then the  $v$ -gap metric is applied in order to pick out a sample model among the models associated with some power levels, and therefore the number of controllers are reduced to three ones for lower power range, mid-power range, and higher power range.

A linear quadratic regulator (LQR) control approach is addressed in Ref. [20] such that the  $H_\infty$ -synthesis is used for ensuring the stability and the tracking capability of the controlled plant at different power demands. This proposed LQR method is employed to adopt the constraints on feed water flowrate. In Ref. [21] a robust control method based on a multi-model predictive control scheme has been developed over the entire operating range from 0% to 100%. In Ref. [22], an optimal tracking control is addressed using the state estimator for the SG water level system considering the power demand variation. Its main aim is to determine the characteristic polynomial for satisfying the stability and robustness necessities of the plant. The non-minimum phase property of the SG and its nonlinear characteristic cause that the reverse thermal-dynamic effect known as “shrinking” and “swelling” make a difficult problem for the system control [23].

The most pervious articles are focused on the methods that are based on gain-scheduling approach where a satisfactory performance may be achieved, however, they cannot guarantee the overall robust stability of the system. They are also established on some different controllers instead of a fixed controller that may causes an unanticipated behavior in switching intervals. The main contribution of this article is presentation of a fixed robust controller for the SG water level system over the whole range of power level deviations. In this paper, the  $\mu$ -synthesis is employed to design the proposed controller. The parameter uncertainties of the SG dynamics, caused by operating power variation, are modeled as multiplicative perturbations which are normalized by appropriate weighting functions. The SG model with the parameters given at 100% plant operating power level is considered as nominal plant model, and its relative error with respect to the SG models with the parameters given at other operating power levels are utilized to determine the weighting functions for normalizing the system uncertainties. Therefore, the general robust control configuration is extracted that can be used for robust synthesis and analysis. The robust analysis ability of the obtained configuration may be useful for certifying the robustness of the existing UTSG controllers against the operating power level deviation. Then a robust controller is driven based on  $\mu$ -synthesis and D-K iteration to achieve the desired performance, stability, and robustness of the SG water level system in the existence of the swell-shrink phenomenon, mechanical oscillations, and steam flowrate variations. Simulation outcomes are given to show the performance of the

suggested controller in comparison with the other regarding controllers such as gain-scheduled  $H_\infty$  controller, QFT controller proposed in Ref. [11], and DSMC suggested in Ref. [9]. The robustness validation ability of the proposed configuration is also implemented for the mentioned controllers.

The rest of the paper is prepared as follows. Section 2 presents the UTSG system model and problem formulation. In third section, the parametric uncertainties due of the plant operating power level change are modeled as multiplicative perturbation. The design procedure of the proposed robust controller is described in Section 4. The simulation results and discussion on controller performance is given in Section 5, and finally Section 6 concludes the paper.

## 2. UTSG system model and problem formulation

In pressurized water reactors (PWRs), the generated energy has been absorbed by the primary coolant. The heated water is pumped to the reactor core and it flows to the SG. The thermal energy of the hot water is exchanged to a secondary system via several equivalent inverted vertical U-tubes. The steam, generated in the secondary system, flows to rotate the turbine of an electric generator. Due of performing daily load cycling operation, the water level variations of the SG may result in serious consequences containing unpremeditated shutting down and system damage. Therefore, the water level should be preserved within its definite range. The problem of maintaining the water level in a constant set point through the variations of the power demand, is hard because the SG has: non-linear behavior, inconstant parameters, restrictions on control effort, water level limitation, and highly measurement noise.

The principle of fluid flow in a UTSG is depicted in Fig. 1. The UTSG is comprised of down-comer, tube bundle, riser, steam separator and steam dome. The feed-water transported from the down-comer to tube bundles. The generated heat of the reactor is absorbed by the rising water by the tube bundle and converted to two-phase mixture. The saturated mixture flows from the lower to upper part of the dryer to be separated into steam and water phases. Finally, the steam is removed by the main steam line. This steam is sent to the turbine for rotating the electric generator. The produced electric power is a function of the steam flow rate entering the turbine. The steam flow rate should be increased by growth of the power demand. This condition alters the steam generator water level.

In a regulation problem of the UTSG water level, feed water

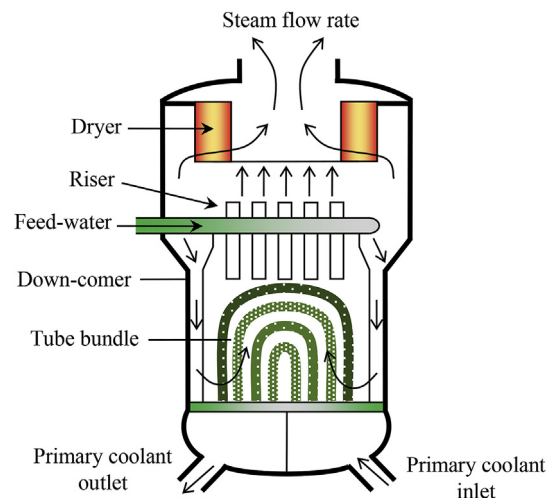


Fig. 1. A cutaway view of UTSG.

flowrate is the control input and steam flowrate is the disturbance input that is arisen mostly by turbine control systems, and water level is the system output. A complete model of UTSG is highly complicated that would require the utilizing of unsteady equations of the mass and energy conservation. Mostly, the simpler models would be sufficed for the control study purposes. The water level model developed by Irving et al.'s [1] can be presented as:

$$\ell = P_1(s)u + P_2(s)(u - d) \quad (1)$$

where,

$$P_1(s) := \frac{G_3s}{\tau_1^{-2} + 4\pi^2T^{-2} + 2\tau_1^{-1}s + s^2}, \quad P_2(s) := \frac{G_1}{s} - \frac{G_2}{1 + \tau_2s} \quad (2)$$

and;  $\ell$  is narrow range water level (mm);  $u$  is feed water flowrate (kg/sec);  $d$  is steam flowrate (kg/sec);  $\tau_1$  and  $\tau_2$  are damping time constants (sec);  $T$  is the mechanical oscillation period (sec);  $G_1$  is the mass capacity effect of the SG (mm/kg);  $G_2$  is the swell and shrink effect value (mm-sec/kg);  $G_3$  is the amount of the oscillation from mechanical effects (mm/kg); and  $s$  is the complex Laplace transform variable.

The parameters of the model at different power operation levels, specified from the experimental data, are presented in Table 1. Several operating power levels ranging are considered from 5% to 100% [1]. This table shows that all of the parameters except  $G_1$  are varied with the power level variations.

A robust controller utilizing  $\mu$ -synthesis is designed to meet the stability and performance requirements. The water level model (1) in a standard feedback control block diagram can be considered as shown in Fig. 2. In this diagram  $P_{10}(s)$  and  $P_{20}(s)$  are the nominal models of  $P_1(s)$  and  $P_2(s)$ , respectively. This nominal models are specified in the 100% power level case. The proper transfer functions  $W_1(s)$  and  $W_2(s)$  are stable and minimum phase as weighting functions for normalizing the plant uncertainties  $\Delta_1(s)$  and  $\Delta_2(s)$  to be less than one in magnitude at each frequency. The transfer function  $W_p(s)$  is defined to weight the desired performance of the system at each frequency. Now the control objective can be stated as to find the robust controller  $K(s)$  which neutralizes the influence of  $d$  on  $z$  in the presence of system uncertainties, thereby minimizing the closed-loop  $\mu$ -norm from  $d$  to  $z$ .

### 3. Modeling of parametric uncertainties

In order to design the controller  $K(s)$ , the uncertainties of the SG are extracted as blocks  $\Delta_1(s)$  and  $\Delta_2(s)$ . The weighting functions  $W_i(s)$ , for  $i = 1, 2$ , fixed stable transfer functions, are used to normalize the uncertain stable transfer functions  $\Delta_i(s)$ , i.e.,  $\|\Delta_i\| \leq 1$  according to the following relation between the nominal systems and the perturbed system.

$$P_i(s) = P_{i0}(s)[1 + \Delta_i(s)W_i(s)] \text{ for } i = 1, 2 \quad (3)$$

Using  $\|\Delta_i(s)\| \leq 1$  implies that

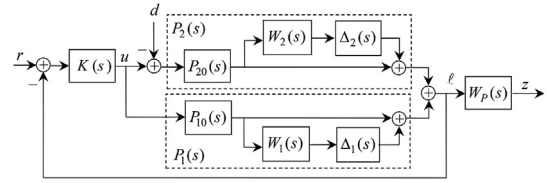


Fig. 2. Considering control structure for uncertainty modeling and control synthesis.

$$L_i(\omega) \leq |W_i(j\omega)|, \quad \forall \omega \text{ for } i = 1, 2 \quad (4)$$

where  $L_i(\omega)$  is the relative error which is defined by

$$L_i(\omega) := \left| \frac{P_i(j\omega) - P_{i0}(j\omega)}{P_{i0}(j\omega)} \right| \text{ for } i = 1, 2 \quad (5)$$

The parametric variations, as presented in Table 1, together with some extra variation associated with different power levels are utilized to generate ten perturbed model systems for  $P_1(s)$  and  $P_2(s)$ . According to (4),  $|W_i(j\omega)|$  should be designed as an upper bound for relative error  $L_i(\omega)$ . The weighting functions  $W_i(s)$  are determined from (4) by choosing a transfer function that is stable and minimum phase, such that the relative errors (5) are covered for all the perturbed models. The relative error of each model and the resulted weighting functions are depicted in Fig. 3 and Fig. 4. As can be seen, the obtained weighting functions, described by the following equations, cover all errors curves and acts as suitable upper bounds for them.

$$W_1(s) = \frac{2.375s^2 + 2.083s + 3.032}{s^2 + 0.172s + 0.0153}, \quad W_2(s) = \frac{3.766s^2 + 1.58s + 8.6 \times 10^{-5}}{s^2 + 0.527s + 0.0086} \quad (6)$$

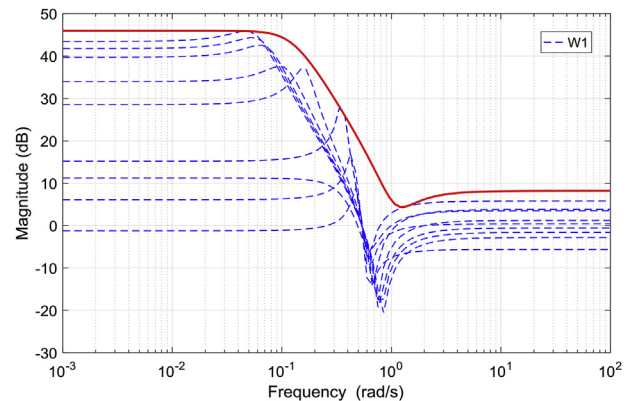


Fig. 3. Relative error plots and resulted weighting function for  $P_1(s)$ .

Table 1  
SG parameters at several operating power levels [1].

Power Level (%)	$G_1$ (mm/kg)	$G_2$ (mm-s/kg)	$G_3$ (mm/kg)	$T$ (sec)	$\tau_1$ (sec)	$\tau_2$ (sec)	$D$ (kg/sec)
5	0.058	9.63	0.181	119.6	41.9	48.4	57.4
15	0.058	4.46	0.226	60.5	26.3	21.5	180.8
30	0.058	1.83	0.310	17.7	43.4	4.5	381.8
50	0.058	1.05	0.215	14.2	34.8	3.6	660.0
100	0.058	0.47	0.105	11.7	28.6	3.4	1434.7

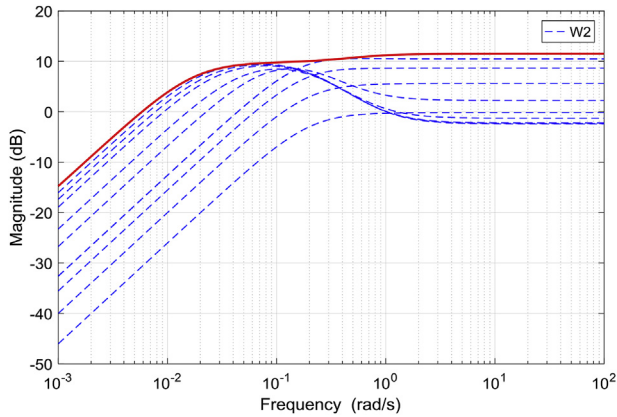


Fig. 4. Relative error plots and resulted weighting function for  $P_2(s)$ .

#### 4. Robust controller design

##### 4.1. $\mu$ -controller design

The control structure in Fig. 2, is represented in general standard block diagram of a robust control problem as Fig. 5 for  $r = 0$ , where  $\Delta(s) = \text{diag}\{\Delta_1(s), \Delta_2(s)\}$ , and

$$P(s) = \begin{bmatrix} 0 & 0 & 0 & P_{10}W_1 \\ 0 & 0 & -P_{20}W_2 & P_{20}W_2 \\ W_p & W_p & -W_pP_{20} & W_pP_{30} \\ -1 & -1 & P_{20} & -P_{30} \end{bmatrix} \quad (7)$$

and,  $P_{30}(s) := P_{10}(s) + P_{20}(s)$ .

The controller  $K(s)$  with combination of plant  $P(s)$  via the lower loop make the following  $N - \Delta$  structure shown in Fig. 6.

According to the configuration shown in Fig. 6, The transfer

$$K(s) = \frac{1.205s^5 + 0.7179s^4 + 0.09953s^3 + 0.00148s^2 + 5.163 \times 10^{-7}s - 3.019 \times 10^{-17}}{s^6 + 1556s^5 + 126.2s^4 + 3.266s^3 + 0.0261s^2 + 9.101 \times 10^{-6}s + 1.413 \times 10^{-14}} \quad (11)$$

function matrix  $N(s)$  is determined with respect to  $P(s)$  and  $K(s)$  by the following lower linear fractional transformation (LFT) that is used later for  $\mu$ -analysis of a given controller  $K(s)$ .

$$N = F_\ell(P, K) = \begin{bmatrix} N_{11} & N_{112} \\ N_{21} & N_{22} \end{bmatrix} = \begin{bmatrix} -P_{10}W_1KS & -P_{10}W_1KS & P_{10}P_{20}W_1KS \\ -P_{20}W_2KS & -P_{20}W_2KS & -P_{10}P_{20}W_2KS \\ W_pS & W_pS & -W_pSP_{20} \end{bmatrix} \quad (8)$$

where,  $S := (1 + P_{30}K)^{-1}$  is the sensitivity function and the Laplace variable  $s$  is omitted for simplicity. The  $\mu$ -synthesis with using the

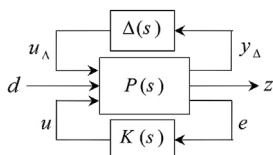


Fig. 5. Standard representation of robust control problem.

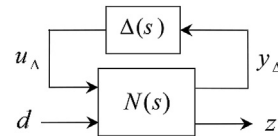


Fig. 6. System configuration in  $N - \Delta$  structure.

structure singular values is an effective tool in robust control problems associated with structured uncertainty. The control objective of the  $\mu$ -synthesis is to find the controller  $K(s)$  such that the following condition is satisfied at each frequency.

$$\mu[F_\ell(P, K)(j\omega)] \leq 1 \quad (9)$$

The D-K iteration is used for solving the above  $\mu$ -synthesis control problem [24,25]. It combines  $H_\infty$ -analysis and  $\mu$ -synthesis, and often yields good results. The robustness of the controller is guaranteed by  $H_\infty$ -analysis and  $\mu$ -synthesis put into consideration the system uncertainty.

To solve problem (9), the weighting function  $W_p(s)$  should be revealed. The weighting function  $W_p(s)$  that is known as a performance weighting function, weights a region of frequency domain to decrease the effect of disturbance  $d$  on the system output. The following weighting function is used to satisfy the solving conditions of the problem.

$$W_p = \frac{0.001s + 1}{s + 7.1} \quad (10)$$

Using D-K iteration, a 19<sup>th</sup> order robust controller is carried out. Because of high order of the resulted controller, a balanced model truncation via square root method [26], is applied for reducing the order of the controller. The resulted 6th order controller with multiplicative error band  $1.18 \times 10^{-4}$  is obtained as

##### 4.2. Gain-scheduled $H_\infty$ controller design

For evaluating the efficiency of the proposed controller, a gain-scheduled controller is designed in this section using  $H_\infty$ -synthesis. Five  $H_\infty$  mixed-sensitivity controllers are designed for the nominal models of the plant at power levels indicated in Table 1. Since the system has a pole at origin, the conventional  $H_\infty$  synthesis is encountered with the problem of  $H_\infty$  condition satisfaction. Therefore, the origin pole is shifted to  $-0.001$  in controller synthesis stage. According to the standard manner in  $H_\infty$  mixed-sensitivity synthesis the control configuration of Fig. 2 is augmented with weighting functions  $W_e(s)$ ,  $W_u(s)$ , and  $W_l(s)$  for considering some penalties on the error signal, control signal and output signal respectively. The control formation of the augmented plant is shown in Fig. 7.

The weighting functions are designed as:

$$W_e(s) = \frac{10(s + 10)}{1000s + 1}, \quad W_u(s) = 200, \quad W_l(s) = \frac{10(s + .01)}{s + 10} \quad (12)$$

Computing a controller that minimizes the  $H_\infty$  norm of the

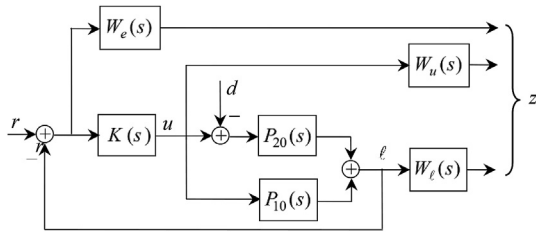


Fig. 7. Augmented plant for  $H_\infty$  mixed-sensitivity synthesis.

weighted mixed sensitivity transfer function from  $r$  to  $z$ , results in the following controllers  $K_1(s)$  to  $K_5(s)$  at five different plant operating power levels 5%, 15%, 30%, 50%, and 100% respectively.

$$K_1(s) = \frac{5.2s^5 + 52.36s^4 + 3.631s^3 + 0.2283s^2 + 0.0038s + 3.577 \times 10^{-6}}{s^6 + 49.92s^5 + 402s^4 + 28.4s^3 + 2.033s^2 + 0.06245s + 6.053 \times 10^{-5}} \quad (13)$$

$$K_2(s) = \frac{0.8364s^5 + 8.468s^4 + 1.047s^3 + 0.1334s^2 + 0.004891s + 4.758 \times 10^{-6}}{s^6 + 18.13s^5 + 82.27s^4 + 10s^3 + 1.327s^2 + 0.06784s + 6.652 \times 10^{-5}} \quad (14)$$

$$K_3(s) = \frac{2.45s^5 + 25.16s^4 + 6.933s^3 + 3.427s^2 + 0.6923s + 6.889 \times 10^{-4}}{s^6 + 36.67s^5 + 274.2s^4 + 78.36s^3 + 36.12s^2 + 8.721s + 8.685 \times 10^{-3}} \quad (15)$$

$$K_4(s) = \frac{0.6391s^5 + 6.606s^4 + 2.285s^3 + 1.396s^2 + 0.3504s + 3.49 \times 10^{-4}}{s^6 + 17.48s^5 + 77.45s^4 + 28.18s^3 + 15.91s^2 + 4.283s + 4.267 \times 10^{-3}} \quad (16)$$

$$K_5(s) = \frac{0.5748s^5 + 5.958s^4 + 2.277s^3 + 1.834s^2 + 0.4914s + 4.896 \times 10^{-4}}{s^6 + 16.96s^5 + 72.37s^4 + 29.5s^3 + 21.81s^2 + 5.872s + 5.85 \times 10^{-3}} \quad (17)$$

By measuring the steam flowrate  $d$ , and comparing with last column of Table 1, the following interpolated controlled is achieved.

$$K(s) = \begin{cases} K_1(s) & \text{if } d \leq d_1 \\ \frac{d_2 - d}{d_2 - d_1} K_1(s) + \frac{d - d_1}{d_2 - d_1} K_2(s) & \text{if } d_1 < d \leq d_2 \\ \frac{d_3 - d}{d_3 - d_2} K_2(s) + \frac{d - d_2}{d_3 - d_2} K_3(s) & \text{if } d_2 < d \leq d_3 \\ \frac{d_4 - d}{d_4 - d_3} K_3(s) + \frac{d - d_3}{d_4 - d_3} K_4(s) & \text{if } d_3 < d \leq d_4 \\ \frac{d_5 - d}{d_5 - d_4} K_4(s) + \frac{d - d_4}{d_5 - d_4} K_5(s) & \text{if } d_4 < d \leq d_5 \end{cases} \quad (18)$$

where,  $d_1$  to  $d_5$  are the steam flowrate at operating points shown in Table 1.

### 4.3. Stability robustness analysis

The stability robustness of the UTSG is analyzed against the parameter uncertainties caused by operating power variation. For this purpose, the parameter uncertainties of the plant are modeled as Fig. 2 in accord with Section 3. Then, the  $N - \Delta$  structure of the system, Fig. 6, is realized by (8). Hence, the robust stability of the UTSG is verified by the following condition.

$$\mu[N_{11}(j\omega)] < 1, \quad \forall \omega \quad (19)$$

Fig. 8 shows the resulting  $\mu$ -curve for both  $\mu$ -controller and gain-scheduled  $H_\infty$  controller. Note that, since the designed  $H_\infty$  controller is a gain-scheduled controller, it has different  $\mu$ -curves up to the power level deviations as shown in Fig. 8. The power level is varied from 1% to 100% and the  $\mu$ -curve of the gain-scheduled  $H_\infty$  controller is drawn for each power level. For robust stability, it is required that the maximum of the  $\mu$ -curves at each frequency (push curve) to be less than unity. It is obvious that the robust stability is not satisfied by the gain-scheduled  $H_\infty$  mixed-sensitivity controller, while the  $\mu$ -curve of the  $\mu$ -controller is less than unity in all frequencies and therefore the robust stability is guaranteed. Fig. 9 shows the robust analysis of the gain-scheduled QFT controller presented in Ref. [11]. The same result can be observed

for this controller.

## 5. Simulation results

The time response of the UTSG with the designed controller is investigated and compared with some existent controllers by simulating the plant with MATLAB/Simulink software. The performance of the suggested controller under the parameter perturbation due of the power level deviation and noisy measurements is evaluated and compared with the gain-scheduled  $H_\infty$  mixed-sensitivity controller, described in Section 4.2, the gain-scheduled QFT-controller, addressed in Ref. [11], that is consist of three QFT-

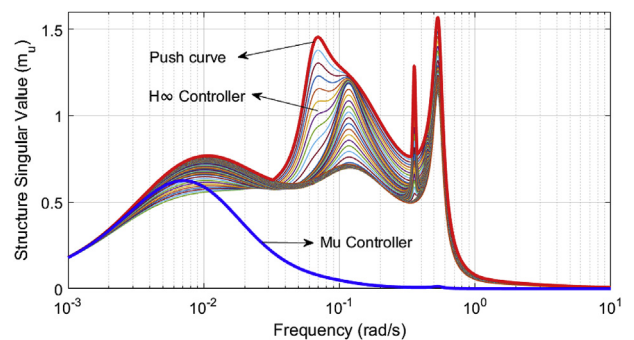


Fig. 8. Structure singular value for stability robustness analysis of  $\mu$ -controller and gain-scheduled  $H_\infty$  controller.

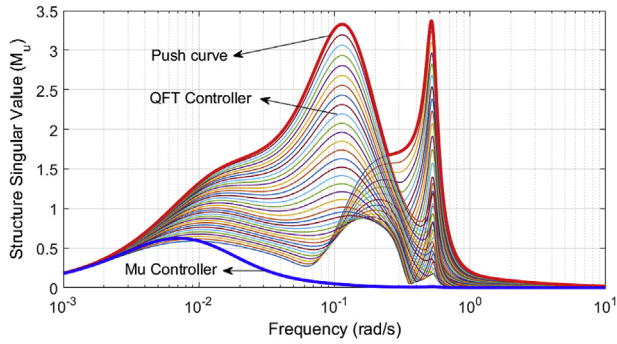


Fig. 9. Structure singular value for stability robustness analysis of  $\mu$ -controller and proposed QFT controller at [11].

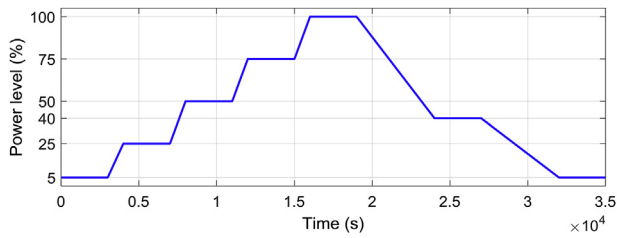


Fig. 10. Power level variation (%).

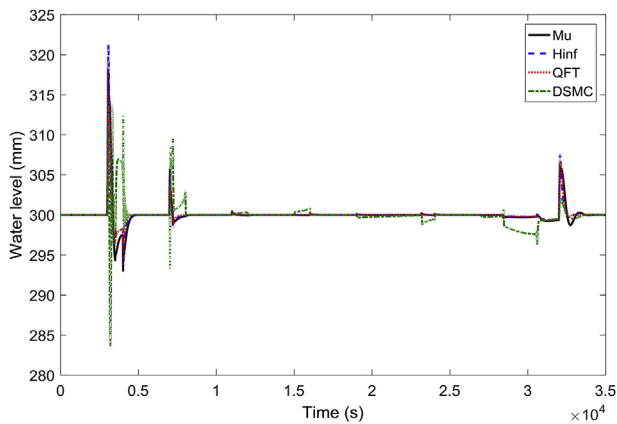


Fig. 11. Water level deviations during power variations with  $\mu$ ,  $H_\infty$ , QFT, and DSMC controllers.

controller at different power levels, and DSMC proposed in Ref. [9]. The operation condition (or accordingly steam flowrate) is varied in whole operation scope from 0% to 100% power level as startup cycle and from 100% to 0% power level as shutdown cycle according to a profile which is displayed in Fig. 10. The water level response without measurement noises are shown in Fig. 11. It can be seen that the output performance of the all controllers are acceptable and there are not significant differences between them. However, a

Table 2  
Comparison of the water level errors with different controllers.

Controllers	Output error norm	
	with measurement noises	without measurement noises
$\mu$	11292	9431
QFT	12031	9844
$H_\infty$	11554	10318
DSMC	27585	24996

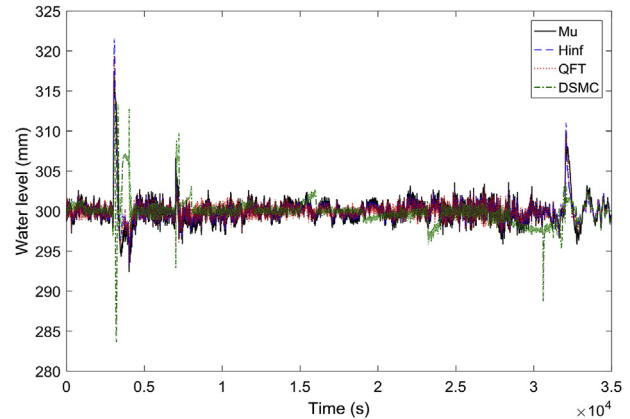


Fig. 12. Water level deviations during power variations with considering the measurement noises.

little improvement can be seen for the plant response with proposed  $\mu$ -controller that is measured by computing 2-norm of the water level error as demonstrated in Table 2. Fig. 12 shows the plant responses when the measurement channels are infected by normally distributed noises with zero mean and standard deviation 10. The norms of the output errors are also exhibited in Table 2. The water level reference signal is assumed to be 300 mm. One of the most important feature of the proposed controller is its singleness over the whole range of power level operations while the three other controllers are gain-scheduled compensators. The DSMC scheme which is described in Ref. [9], has a suitable performance when the power level is not varied, however in the time intervals that the power level is varying it doesn't show appropriate behavior in comparison with the other controllers. It should be also noted that the DSMC approach is based on the assumption that all the system states are available, while the other use an output feedback measurement.

## 6. Conclusion

In this paper, a  $\mu$ -synthesized robust controller is developed for the UTSG water level system. In the proposed control structure, a unique controller is achieved over the whole scope of power operations instead of multiple and gain-scheduled robust controllers introduced by previous researchers. The multiplicative presentation is used for modeling the parameter uncertainties of the SG dynamics. The relative errors for several operating power levels are utilized to indicate the weighting functions for normalizing the system uncertainties. Therefore, a general robust control configuration is extracted that is used for robust synthesis and robust analysis. The attained configuration is employed for validating the stability robustness of some existing UTSG controllers against the operating power level deviation. The stability robustness analysis shows that the proposed  $\mu$ -synthesis controller fulfils the robust stability condition while the some mentioned regarding controllers such as gain-scheduled  $H_\infty$  controller, QFT controller proposed in Ref. [11], are unsuccessful to satisfy the robust stability condition in  $\mu$ -analysis point of view. Numerical simulations are performed to evaluate the proposed scheme and to compare the controller response with the other controllers. The robustness validation ability of the proposed configuration is also implemented for the mentioned controllers.

## Conflicts of interest

All authors have no conflicts of interest to declare.

## Appendix A. Supplementary data

Supplementary data to this article can be found online at <https://doi.org/10.1016/j.net.2018.09.018>.

## References

- [1] E. Irving, C. Miossec, J. Tassart, Toward efficient full automatic operation of the PWR steam generator with water level adaptive control, in: *Proceeding 2nd Int. Conf. Boil. Dyn. Control Nucl. Power Station*, British Nuclear Energy Society, London, 1980, pp. 309–329.
- [2] S.K. Menon, A.G. Parlos, Gain-scheduled nonlinear control of u-tube steam generator water level, *Nucl. Sci. Eng.* 111 (1992) 294–308, <https://doi.org/10.13182/NSE92-A23942>.
- [3] O. Safarzadeh, A. Khaki-Sedigh, A.S. Shirani, Identification and robust water level control of horizontal steam generators using quantitative feedback theory, *Energy Convers. Manag.* 52 (2011) 3103–3111, <https://doi.org/10.1016/j.enconman.2011.04.023>.
- [4] J.I. Choi, J.E. Meyer, D.D. Lanning, Automatic controller for steam generator water level during low power operation, *Nucl. Eng. Des.* 117 (1989) 263–274, [https://doi.org/10.1016/0029-5493\(89\)90175-1](https://doi.org/10.1016/0029-5493(89)90175-1).
- [5] K.K. Kim, J.E. Meyer, D.D. Lanning, J.A. Bernard, Design and evaluation of model-based compensators for the control of steam generator level, in: *Am. Control Conf.*, 1993, pp. 2055–2060.
- [6] M.V. Kothare, B. Mettler, M. Morari, P. Bendotti, C.M. Falinower, Level control in the steam generator of a nuclear power plant, *IEEE Trans. Contr. Syst. Technol.* 8 (2000) 55–69, <https://doi.org/10.1109/87.817692>.
- [7] M.G. Na, Y.R. Sim, Y.J. Lee, Design of an adaptive predictive controller for steam generators, *IEEE Trans. Nucl. Sci.* 50 (2003) 186–193, <https://doi.org/10.1109/TNS.2002.807854>.
- [8] K. Hu, J. Yuan, Multi-model predictive control method for nuclear steam generator water level, *Energy Convers. Manag.* 49 (2008) 1167–1174, <https://doi.org/10.1016/j.enconman.2007.09.006>.
- [9] G.R. Ansarifard, H.A. Talebi, H. Davilu, Adaptive estimator-based dynamic sliding mode control for the water level of nuclear steam generators, *Prog. Nucl. Energy* 56 (2012) 61–70, <https://doi.org/10.1016/j.pnucene.2011.12.008>.
- [10] W. Tan, Water level control for a nuclear steam generator, *Nucl. Eng. Des.* 241 (2011) 1873–1880, <https://doi.org/10.1016/j.nucengdes.2010.12.010>.
- [11] O. Safarzadeh, A.S. Shirani, Robust water level control of the U-tube steam generator, *J. Energy Eng.* 139 (2013) 161–168, [https://doi.org/10.1061/\(ASCE\)EY.1943-7897.0000107](https://doi.org/10.1061/(ASCE)EY.1943-7897.0000107).
- [12] S.R. Munasinghe, M.S. Kim, J.J. Lee, Adaptive neurofuzzy controller to regulate UTSG water level in nuclear power plants, *IEEE Trans. Nucl. Sci.* 52 (2005) 421–429, <https://doi.org/10.1109/TNS.2004.842723>.
- [13] K. Kavaklioglu, Support vector regression model based predictive control of water level of U-tube steam generators, *Nucl. Eng. Des.* 278 (2014) 651–660, <https://doi.org/10.1016/j.nucengdes.2014.08.018>.
- [14] A. Fakhrazari, M. Boroushaki, Adaptive critic-based neurofuzzy controller for the steam generator water level, *IEEE Trans. Nucl. Sci.* 55 (2008) 1678–1685, <https://doi.org/10.1109/TNS.2008.924058>.
- [15] M.G. Na, Design of a genetic fuzzy controller for the nuclear steam generator water level control, *IEEE Trans. Nucl. Sci.* 45 (1998) 2261–2271, <https://doi.org/10.1109/23.709657>.
- [16] H. Habibiyan, S. Setayeshi, H. Arab-Alibeik, A fuzzy-gain-scheduled neural controller for nuclear steam generators, *Ann. Nucl. Energy* 31 (2004) 1765–1781, <https://doi.org/10.1016/j.anucene.2004.03.014>.
- [17] S. Beyhan, K. Kavaklioglu, Comprehensive modeling of U-tube steam generators using extreme learning machines, *IEEE Trans. Nucl. Sci.* 62 (2015) 2245–2254, <https://doi.org/10.1109/TNS.2015.2462126>.
- [18] A.G. Parlos, O.T. Rais, Nonlinear control of U-tube steam generators via H<sub>∞</sub> control, *Contr. Eng. Pract.* 8 (2000) 921–936, [https://doi.org/10.1016/S0967-0661\(00\)00020-4](https://doi.org/10.1016/S0967-0661(00)00020-4).
- [19] J.J. Sohn, P.H. Seong, A steam generator model identification and robust H<sub>∞</sub> controller design with v-gap metric for a feedwater control system, *Ann. Nucl. Energy* 37 (2010) 180–195, <https://doi.org/10.1016/j.anucene.2009.11.005>.
- [20] L. Wei, F. Fang, H<sub>∞</sub>-based LQR water level control for nuclear U-tube steam generators, in: *Control Decis. Conf.*, 2013, pp. 4076–4080.
- [21] A. Osgouee, J. Jiang, Robust nonlinear method for steam generator level control, *Nucl. Technol.* 181 (2013) 493–506, <https://doi.org/10.13182/NT13-A15806>.
- [22] G. Ablay, A robust estimator-based optimal algebraic approach to steam generator feedwater control system, *Turk. J. Electr. Eng. Comput. Sci.* 24 (2016) 206–218, <https://doi.org/10.3906/elk-1307-46>.
- [23] Z. Gang, P. Wei, Z. Dafa, Analysis of water level control methods for nuclear steam generator, *At. ENERGY Sci. Technol.* (2004) 19–23.
- [24] S. Skogestad, I. Postlethwaite, *Multivariable Feedback Control: Analysis and Design*, second ed., Wiley, New York, 2005.
- [25] G.J. Balas, J.C. Doyle, K. Glover, A. Packard, R. Smith, *M-analysis and Synthesis Toolbox*, MUSYN Inc. MathWorks, Natick MA, 1993.
- [26] K. Glover, All optimal Hankel-norm approximations of linear multivariable systems and their L<sub>∞</sub>-error bounds, *Int. J. Contr.* 39 (1984) 1115–1193, <https://doi.org/10.1080/00207178408933239>.